

A novel MPPT design for a wind energy conversion system using grey wolf optimization

G. Rashmi & M. Mary Linda

To cite this article: G. Rashmi & M. Mary Linda (2023) A novel MPPT design for a wind energy conversion system using grey wolf optimization, *Automatika*, 64:4, 798-806, DOI: [10.1080/00051144.2023.2218168](https://doi.org/10.1080/00051144.2023.2218168)

To link to this article: <https://doi.org/10.1080/00051144.2023.2218168>



© 2023 The Author(s). Published by Informa UK Limited, trading as Taylor & Francis Group



Published online: 09 Jun 2023.



Submit your article to this journal [↗](#)



Article views: 431



View related articles [↗](#)



View Crossmark data [↗](#)



A novel MPPT design for a wind energy conversion system using grey wolf optimization

G. Rashmi^a and M. Mary Linda^b

^aDepartment of EEE, Ponjesly College of Engineering, Nagercoil, India; ^bDepartment of EEE, Arunachala College of Engineering for Women, Nagercoil, India

ABSTRACT

A significant problem is enhancing the reliability of the wind energy conversion system (WECS), when that runs in unpredictable weather. Therefore, it is essential to construct a maximum power point tracker (MPPT), a controller for measuring the optimum power that the WECS is expected to generate. Hill climbing-based techniques were used to simulate the tracker, but they had drawbacks in terms of tracking efficiency and speed. The Grey Wolf optimization algorithm (GWO) for modelling MPPT integrated with the WECS is proposed in this work as a novel, effective method. The system is made up of a wind turbine (WT) conjoined to a permanent magnet synchronous generator (PMSG), a 3-phase rectifier that converts the generator's AC output power to direct current (DC), and a boost converter whose input DC voltage is controlled by the MOSFET duty cycle. The goal of the modelling procedure is the system's electrical output power, which is presented as an optimization problem. The results confirmed the GWO-reliability MPPT's in reaching the desired WECS performance.

ARTICLE HISTORY

Received 22 February 2023
Accepted 20 May 2023

KEYWORDS

Grey wolf optimization (GWO); wind energy conversion system (WECS); permanent magnet synchronous generator (PMSG); maximum power point tracker (MPPT)

1. Introduction

The combustion of biofuels to produce power today has had an effect on the Earth's ecosystem and its inhabitants. Due to these effects and the increasing decrease in the supply of biofuels, WECS have been developed to utilize wind as a substitute energy source to fulfil the energy requirements. The systems are efficient and environmentally beneficial, integrating them into the current electricity infrastructures still poses significant difficulties. This is a result of the wind's inherent unpredictability. Wind speed variations make it challenging to keep WECS generation and power demand in balance and lead to energy oscillations in the electrical network. As a result, the grid's voltage and frequency may operate outside the permitted bounds. To minimize this effect, the MPPT for WECS and grid electric power can be adjusted using an energy storage system (ESS).

The mechanical energy of a WT, that would be connected to the drive through a gear box, is used in a WECS to generate electrical power. The load turns the rotor of the generator while it is linked to the winding of the stationary part. The mechanical energy from a wind turbine could be modified within the required wind speeds, which spans from cut-in-speed (V_{cut-in}) to a cut-out-speed ($V_{cut-out}$). Indeed of safety reasons, the primary mover shouldn't work whenever the speed of the wind is outside of designated range. The generator,

the WT and the power stage are typical components of WECS systems.

Wind generation systems with fixed and variable speeds are the two primary categories of WECS (WGS). The only wind turbines that can produce the most power are those with changeable wind speeds. A power converter should be installed in this type of turbine to regulate the energy flow; this will monitor the MPPT. WTs with variable speeds can adjust their rotational speed to match variations in wind speed. The WECS depending on a PMSG has lately grown in favour and has seen a rapid rise in application in large WT generators for variable speed WGS. Its expansion is influenced by a variety of elements, such as less mechanical stress, improved performance, better energy per weight and increased dependability.

The WECS efficiency is fairly significant since the initial cost of the WECS is a significant component in investments. An effective WECS will be one that is operated at full power at all times. MPPT is the term used in the literature to describe it. It is feasible to use the WECSs at changing speeds due to the nonlinear dynamics of the devices and the unpredictability of the wind speed. The adoption of PMSG in this experiment was motivated by these advantages. The experts' 2 major choices for WECS applications based on PMSG are rectifier – DC-DC converter topologies and back-to-back converter (BTBC) topologies. However, when

efficiency and cost are taken into account, the uncontrolled rectifier as well as Boost converter (BC) designs are often desired for both average and small sized WECS.

The reason the authors chose this topology for their research is that it enables the most effective and simple use of control techniques for the purpose of switching the BC to collect the energy possible from the WECS. In two important portions of the literature, the MPPT operation for WECS is mostly covered. The first section covers various MPPT search techniques with the goal of locating the best operating point. The second, however, is concerned with the controller designs that, by creating the power converter switching signals, brought the system to this position.

Furthermore, these two research areas are crucial since they influence how effective WECS is. Direct and indirect power control methods are the two basic classes that can be used to categorize the first category, MPPT methods. IPCs have pre-requisites like sensor, mathematics and learning expertise, whereas DPCs don't need mechanical sensors or prior knowledge. The most popular DPCs are the Optimum Relation Based (ORB), Perturbation and Observation (P&O) and Incremental Conductance (IC) techniques.

In this work, it is suggested that the global MPP be recovered utilizing a Grey Wolf optimal adaptive fuzzy logic controlled (ALFC) technique. The objective is to enhance the MPP tracking and performance of the WECS at all uniform as well as non-uniform speeds. The proposed AFLC uses the GWO methodology to tune the scaling factors of the MFs of the FLC. Scaling factor optimization aims to decrease steady state error and increase responsiveness.

A lot of research has been done in modelling the MPPT for WECS. The majority used standard algorithm such as P&O and improved P&O, while some others utilized metaheuristic optimization methods to optimize the proportional integral (PI) control system or the artificial neural network (ANN)-based controllers. Sitharthan et al. [1] demonstrated an improved particle swarm optimizer (PSO) for modelling the MPPT of a doubly fed induction generator powered by wind energy. In addition to the updated optimizer, the researchers used an ANN with a radial basis function. Kumar et al. [2] conducted a comparison research of two alternative hybrid solar/wind system techniques, P&O and HCS.

Priyadarshi et al. [3] utilized an ant colony optimizer to simulate the MPPT along with a hybrid solar/wind system in order to increase its output power. Furthermore, instead of the traditional PI controller, Fuzzy logic control (FLC) was used to inverter control. Certain issues associated with WECS were eliminated by implementing a new MPPT tactics based on adaptable active fault tolerant influence [4]. Ghoulbourk

et al. [5] created a fractional control mechanism for modifying the pitch angle of a wind energy system in order to maximize the power output. Furthermore, comparisons with the PI and PIA controllers have been made.

Kumar et al. [6] examined numerous methods used in modelling the MPPT for wind power systems, emphasizing its advantages and disadvantages. Brasil et al. [7] built a model of a grid-connected WECS, and FLC for MPPT was added to maximize system output power. To improve the efficiency of hybrid fuel cell/photovoltaic/wind energy, Fathabadi et al. [8] described about a universal tracker. Three different sensors are needed to measure the endpoint voltages of three sources of power without the need for more expensive sensors such as an anemometer and a tachometer. As a control approach for maximizing the power supplied by a wind energy producing system, a neural network with a radial basis function was proposed [9].

Zholtayev et al. [10] developed model predictive control (MPC) using MPPT to obtain the most power from a WECS. Mokhtari et al. [11] built an MPPT for a wind energy system utilizing a PI controller optimized with an ant colony optimizer to improve the controller's tracking speed. To maximize the wind system output power, a novel control based on MPPT pitch angle was implemented using a neural network [12]. Linfei Yin and Qi Gao [13] introduces two MPPT methodologies, tip speed ratio and optimum torque control, for use with wind energy systems. Li et al. [14] suggested a hybrid method for simulating MPPT for wind energy systems that combines HCS and power signal feedback control. Bekakra et al. proposed a PI controller optimized using PSO [15].

Regardless of the huge number of surveyed approaches for modelling MPPT with WECS, the use of metaheuristic algorithms was still limited and requires more attention, particularly after they demonstrated high performance in obtaining the maximum power point (MPP) of wind energy systems. Furthermore, hill climbing search algorithms have certain constraints in terms of tracking speed and efficiency, and they may fail to extract the MPP [16].

To fill the space left by the preceding methods, an efficient metaheuristic strategy based on the GWO is suggested to construct MPPT installed with PMSG driven by WT. GWO is distinguished by its simple implementation, which necessitates fewer regulating factors. Furthermore, AOA convergence can be controlled by assigning at random and adaptable parameters. Furthermore, it accomplishes equilibrium among the mining and extraction phases, allowing the model to achieve global optimization.

This study's key contribution can be summed up as follows:

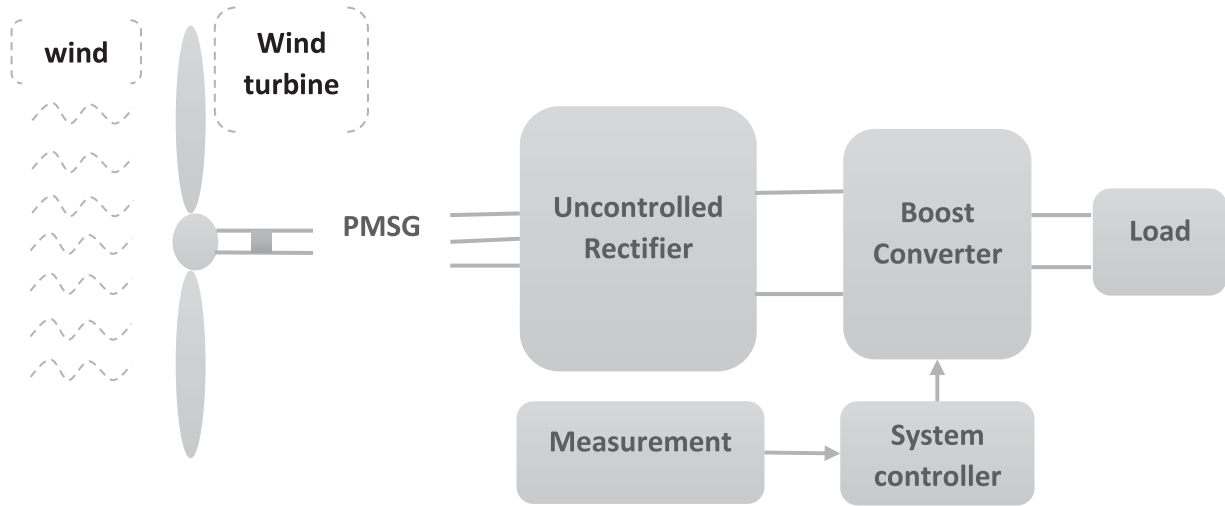


Figure 1. WECS configuration based on PMSG.

- The effectiveness of the recommended MPPT algorithm is enhanced by adding several components to the usual GSS technique, such as detecting the fluctuation in speed of the wind, dynamic uncertain rate and reducing fluctuation among the highest power point.
- The effectiveness of the suggested strategy is examined for realistic and step-type wind speed profiles. Comparative tests for various wind-speed profiles provide to support the suggested method's superiority over variable speed P&O and traditional P&O approaches.
- On the planned test setup, an experimental investigation is also done to determine how well the proposed method performs in real-time when the wind speed varies step-by-step.

Here is the remainder of the paper. The WECS configuration as well as modelling utilized in this article are depicted in Section 2. Section 3 contains information on the Grey Wolf Optimization for MPPT Design. Sections 4 and 5 offer the simulation's results as well as related discussion and conclusions.

2. WECS configuration and modelling

The components of the small-scale WECS include a wind turbine, a PMSG, an unregulated rectifier, a connecting capacitor, a step-up regulator and a controller [16–20]. This arrangement is recommended in this paper because it offers small-scale applications ease and affordability. Since there is no gearbox needed, the PMSG has a cost advantage and is directly connected to the WT shaft. The MPPT method is used in this architecture by measuring some signals, identifying the BC's ideal input voltage, and then transferring the ideal values to the regulator. The regulator produces the BC's switching signals, which control the PMSG voltage and

Table 1. IEC Wind Classes.

| | I(High Wind) | II(Medium Wind) | III(Low Wind) | IV(Very Low Wind) |
|---------------------|--------------|-----------------|---------------|-------------------|
| Ref. Wind Speed | 50m/s | 42.5m/s | 37.5m/s | 30m/s |
| Avg. Wind Speed | 10m/s | 8.5m/s | 7.5m/s | 6m/s |
| 50-year return gust | 70m/s | 59.5m/s | 52.5m/s | 42m/s |
| 1-year return gust | 52.5m/s | 44.6m/s | 39.4m/s | 2.5m/s31.5 |

enable the controller to harvest the most power possible from the WECS (Figure 1).

The system consists of a WT linked to a PMSG, and a 3-phase rectifier that converts the generator's AC output power to DC. The boost converter is given the DC voltage and current, and the proposed GWO-MPPT controller controls the boost converter. The suggested controller's input data are the electrical energy and the mechanical velocity of the WT, which is determined by a tachometer. The controller's output is the duty cycle. The IEC Wind Classification and the wind velocities that turbine must be built to withstand are listed in Table 1.

The following is a description of the models of each component of the integrated WECS:

2.1. Wind turbine characteristics

The rotational force of the wind impacting the WT blades provides the input power. The following are the mechanical powers that a turbine can generate:

$$P_m = \frac{1}{2} \rho A C_p(\lambda, \beta) V_W^3 \quad (1)$$

where V_W is the speed of air, ρ is the density of air, A is the WT swept area and $C_p(\lambda, \beta)$ is the WT power coefficient made up of λ and β . In the WT with fixed pitch angle ($\beta = 0$), C_p only fluctuates depending on, and λ is specified as follows:

$$\lambda = \frac{\omega_m R}{V_w} \quad (2)$$

By inserting (2) in (1), the mechanical power can be rewritten as follows:

$$P_m = \frac{1}{2} \rho A C_p \left(\frac{\omega_m R}{\lambda} \right)^3 \quad (3)$$

Later, the swept area is changed in (3) so that $A \pi R = 2 A = \pi R^2$ is obtained to produce:

$$P_m = \frac{1}{2} \frac{\rho \pi R^5 C_p}{\lambda^3} \omega_m^3 \quad (4)$$

In this case, if is chosen at the ideal value, C_p is maintained at its maximum value, and P_{m_max} is produced as follows:

$$P_{m_max} = \frac{1}{2} \frac{\rho \pi R^5 C_{pmax}}{\lambda_{opt}^3} \omega_m^3 = K_{p_opt} \omega_m^3 \quad (5)$$

where the constant K_{p_opt} is used. Reaching P_{L_max} cannot be assured, even if P_{m_max} is obtained (Figure 2).

Because the generator transforms the mechanical power of the WT into voltage, which is then rectified by the unregulated rectifier and delivered to the operation point by BC. Here, output power is given as follows, taking into account the generator's efficiency η_{gen} and the power conversion topology η_{conv} :

$$P_L = P_m \eta_{gen} \eta_{conv} \quad (6)$$

But because the losses vary with generator speed, the efficiencies of the converter and generator are not stable. Thus, exact and useful data could be gathered if MPPT effectiveness was assessed from the load side when it gets to the mechanical aspects.

2.2. Characteristics of uncontrolled rectifier and PMSG

PMSG operate self-excited and don't need excitation current in the stator because permanent magnets are built into the rotor. The following is the definition of induced back emf for PMSG and how it relates to rotor speed:

$$E = kp\omega \quad (7)$$

here k is a steady coefficient and p is the number of pole pair. The per phase voltage of a PMSG is expressed as follows in the steady state:

$$V = E - I(R_s + jp\omega L_s) \quad (8)$$

where I is phase current and R_s and L_s are stator phase resistance and inductance. The rectifier output voltage is created when the diode losses are ignored, and is represented as follows:

$$V_{dc} = \frac{3\sqrt{6}}{\pi} V - \frac{3}{\pi} P\omega L_s I_L$$

$$= \frac{3\sqrt{6}}{\pi} (E - I(R_s + jp\omega L_s)) - \frac{3}{\pi} P\omega L_s I_L \quad (9)$$

In case I_L is replaced in (9) as $I_L = \frac{\pi}{\sqrt{6}} I$, V_{dc} is rearranged as follows:

$$V_{dc} = \frac{3\sqrt{6}}{\pi} \left(\sqrt{(kp\omega)^2 - (P\omega L_s I)^2} - IR_s \right) - \frac{3}{\sqrt{6}} P\omega L_s I \quad (10)$$

As shown in (10), V_{dc} changes linearly with ω as shown by:

$$V_{dc} = k_v \omega \quad (11)$$

where, k_v is a convergence constant.

2.3. DC-DC boost converter

As represented in Figure 1, the BC is equipped to receive the output of the three-phase uncontrolled bridge rectifier. Because BC only has one power-switching element, it offers a safer, simpler and easier control than other topologies. At this point, the BC's dynamics should be taken into account as follows:

$$\frac{dV_0}{dt} = \bar{u} \frac{I_L}{C} - \frac{V_0}{RC} \quad (12)$$

$$\frac{dI_L}{dt} = \bar{u} \frac{V_0}{L} - \frac{V_{in}}{L} \quad (13)$$

$$I_C = \bar{u} I_L - \frac{V_0}{R} \quad (14)$$

where V_{in} and V_0 are BC's input and output voltages. I_L and I_C are the currents of inductance and capacitance, respectively. The terms load resistance, capacitance and inductance are R , C & L . Here, u is the control signal, while $\bar{u} = 1 - u$ denotes the inverse control signal. Additionally, d denotes a duty ratio spanning from 0 to 1, and κ is known as the converter ratio of BC, as shown by

$$V_{in} = kV_o, \{k = 1 - d\} \quad (15)$$

3. Grey wolf optimization for MPPT design

The GWO algorithm stimulates the organizational setup and hunting strategies used by grey wolves in the wild. According to legend, grey wolves are the top predators and like to live in packs. The four various breeds of grey wolves used for indicating the leadership hierarchy are alpha (α), beta (β), delta (δ) and omega (ω). To quantitatively represent the wolf social structure, we create GWO and use the fittest solution as the alpha (α). The second and third best answers are therefore called beta (β) and delta (δ), accordingly. It is believed that the remaining potential solutions are all omegas (ω). During a hunt, grey wolves will circle

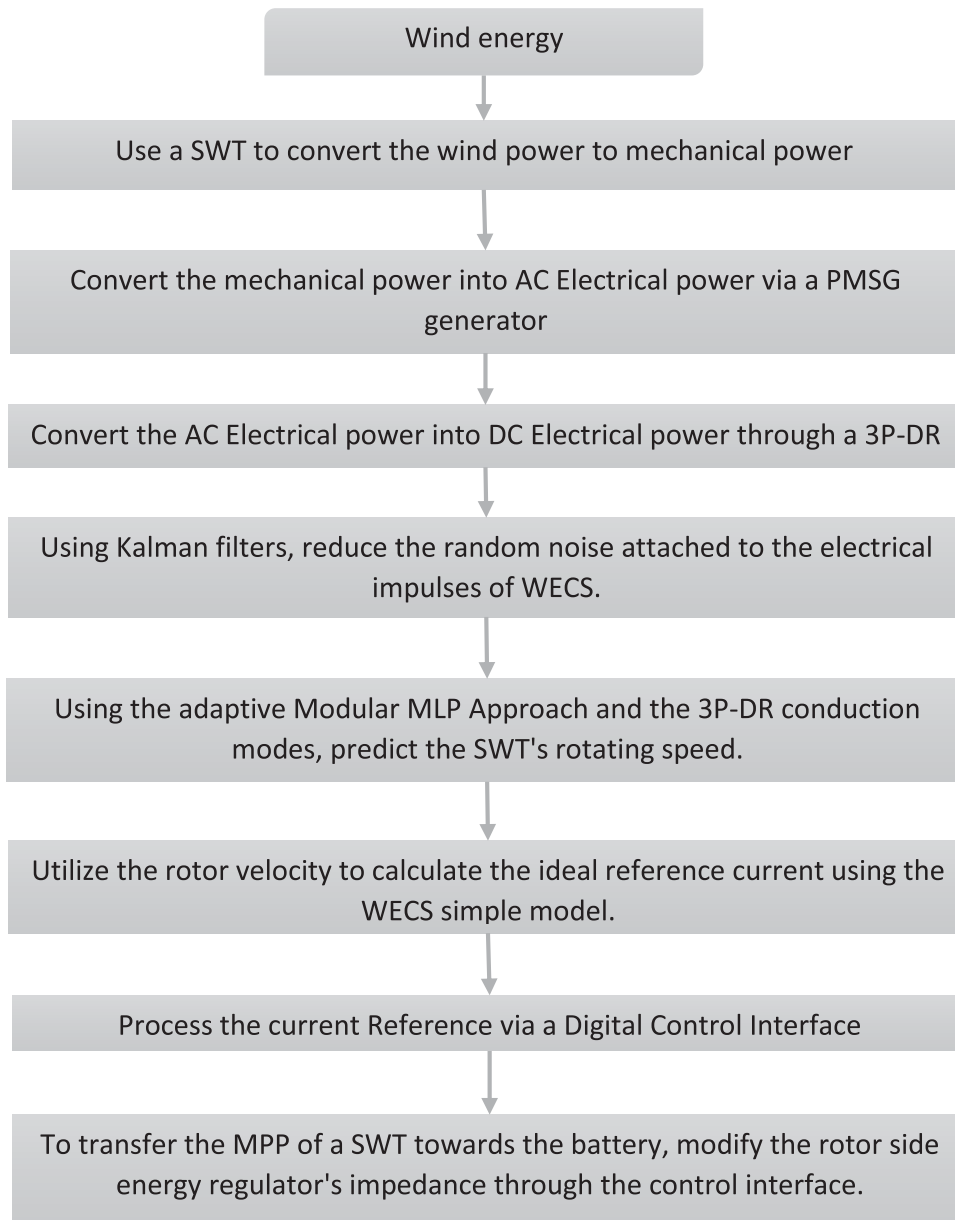


Figure 2. SWT uses the MPPT technique to reach its MPP.

a prey, and the following equations can simulate this behaviour:

$$\vec{D} = \vec{C} \cdot \vec{X}_p(t) - \vec{X}_p(t) \quad (16)$$

$$\vec{X}(t+1) = \vec{X}_p(t) - \vec{A} \cdot \vec{D} \quad (17)$$

where t indicates the current iteration, D , A and C stand for coefficient vectors, X_p is the prey's position vector, and X stands for the grey wolf's position vector. Following are the calculations for the vectors A and C :

$$\vec{A} = 2\vec{a} \cdot \vec{r}_1 - \vec{a} \quad (18)$$

$$\vec{C} = 2 \cdot \vec{r}_2 \quad (19)$$

Where random vectors in the range $[0, 1]$ are denoted as r_1, r_2 and components of a linearly decline from 2 to 0 over the length of iterations. The alpha, sometimes known as the leaders, usually directs the

hunt, with beta and delta occasionally joining in. The injured wolves in the pack are treated by delta (δ), and omega (ω). Alpha (α) is the candidate solution that has a superior understanding of the prey's position. The grey wolves pursue the prey after it stops moving to put an end to the chase.

The duty cycle is kept constant at the MPP, limiting the steady-state oscillation present in traditional MPPT methods, that ultimately reducing the power failure because of fluctuation, resulting in higher system performance. Consequently, (17) can be changed as follows:

$$D_i(k+1) = D_i(k) - A \cdot D \quad (20)$$

Consequently, the GWO algorithm's fitness function is written as

$$P(d_i^k) > P(d_i^{k-1}) \quad (21)$$

In this research, we would employ grey wolf optimization to optimize two fitness functions: Rastrigin and Sphere. The Grey wolf optimization algorithm seeks to minimize the fitness function. The Rastrigin function is a non-convex function that is used to measure the performance of optimization techniques. The presence of several cosine oscillations on the plane creates a plethora of local minimums in which particles can become lodged. The sphere function is used to measure the performance of optimization techniques.

Steps should be followed for fitness value is shown below:

Step 1: Randomly initialize Grey wolf population of N particles X_i ($i = 1, 2, \dots, n$)

Step 2: Calculate the fitness value of each individuals sort grey wolf population based on fitness values $\alpha_{\text{wolf}} = \text{wolf with least fitness value}$

$\beta_{\text{wolf}} = \text{wolf with second least fitness value}$

$\gamma_{\text{wolf}} = \text{wolf with third least fitness value}$

Step 3: For Iter in range (max_iter): # loop max_iter times calculate the value of $a = 2 * (1 - \text{Iter}/\text{max_iter})$ For i in range (N): # for each wolf a .

3.1. GWO algorithm

Hunting: Grey wolves are capable of locating their prey and surrounding it. Generally speaking, the alpha wolf leads the hunt. All search agents change their positions in the mathematical model of grey wolves' hunting behaviour depend on the location of the best candidate solution (a , b and d). The hunting habits of grey wolves are as follows:

$$\vec{D}_\alpha = |\vec{C}_1 \cdot \vec{X}_\alpha - \vec{X}|; \quad (22.a)$$

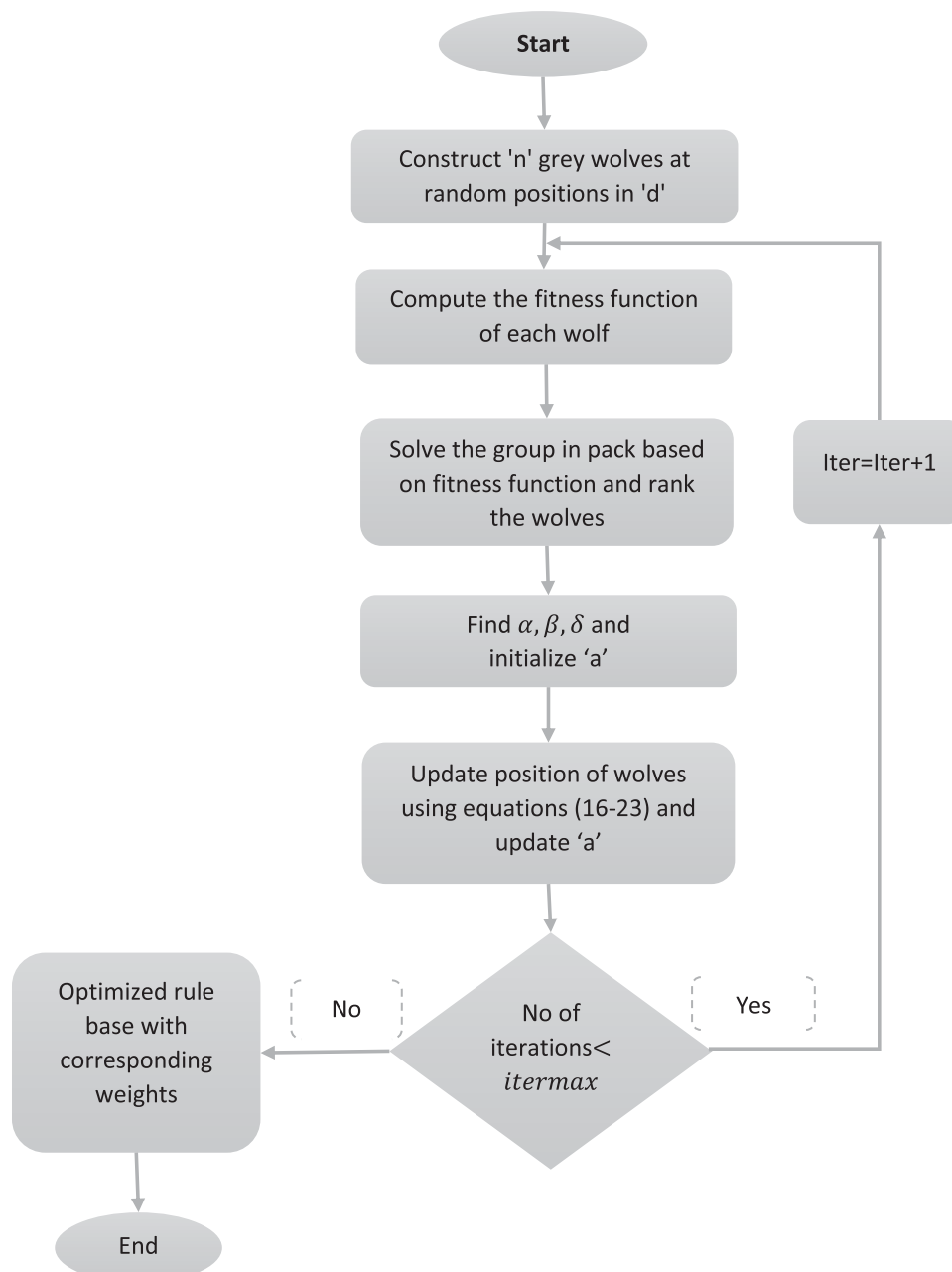


Figure 3. Flowchart of GWO.

$$\vec{D}_\beta = |\vec{C}_1 \cdot \vec{X}_\beta - \vec{X}|; \tag{22.b}$$

$$\vec{D}_\delta = |\vec{C}_1 \cdot \vec{X}_\delta - \vec{X}| \tag{22.c}$$

$$\vec{X}_1 = \vec{X}_\alpha - \vec{A}_1 \cdot (\vec{D}_\alpha); \tag{23.a}$$

$$\vec{X}_2 = \vec{X}_\beta - \vec{A}_2 \cdot (\vec{D}_\beta); \tag{23.b}$$

$$\vec{X}_3 = \vec{X}_\delta - \vec{A}_3 \cdot (\vec{D}_\delta) \tag{23.c}$$

Attacking prey: As was already said, the final step in a grey wolf's hunting procedure is to attack its target once it has stopped moving. Here, the \vec{A} fluctuation range is reduced as \vec{a} . Based on where the α, β and δ wolves are, the GWO algorithm updates the positions of all search agents to attack the prey.

Prey search: While foraging for prey, the grey wolves split up and come together. When the random value (A) is more than 1 or less than 1, the exploring behaviour is more apparent. This enables the GWO algorithm to search the entire world. The GWO method also includes (C), which favours exploration in addition to (A). The value of (C) fluctuates arbitrarily in [0 2]. The search agents were more drawn to the prey when this component is bigger than 1. This supports the GWO's preference for increased exploration and avoiding local optima.

The flowchart for GWO-based adjustment of FLC parameter scaling factors is shown in Figure 3. The subsequent list summarizes the consecutive steps shown in Figure 3:

4. Results and discussion

In this study, three operational conditions under constant, variable and actual wind speeds are examined. Table 2 contains the system specs. The best fitness function among all the optimizers used in this study is

Algorithm 1

Step 1:

Initialization:

Use the below equation to determine the GWO overall population in the beginning:

$$\vec{X}_{ij} = lb + rand * (ub - lb)$$

Where, $lb = [0000]$; $ub = [1111]$;

Step 2:

Fitness assessment:

Each wolf's fitness value should be estimated.

Step 3:

Selection:

Sort the wolves in decreasing order based on how fit they are. The top three wolves in the population are designated as a, b, and d.

Step 4:

Each wolf's location should be updated:

Using Equations (16)–(24), update the wolf population positions.

Step 5:

Termination criteria:

If the termination requirement is met, note the best scaling factors; otherwise, move on to step 2.

Table 2. Wind energy conversion system parameters.

| Unit | Description | Parameter | Nominal value |
|-----------------|-----------------------|--------------|-------------------------|
| Boost Converter | Capacitance | C | 1500 μ F |
| | Inductance | L | 4.5 mH |
| | Inductance resistance | r_l | 0.15 Ω |
| | Load resistance | R_{load} | 150 Ω |
| | switching frequency | f_s | 5kHz |
| PMSG | Friction factor | J | 0.013 kg.m ² |
| | Friction factor | F | 0.0425 N.m.s |
| | Armature Inductance | L_a | 0.000835 H |
| | Stator resistance | R_s | 5 Ω |
| | Pole pairs | P | 8 |
| Wind turbine | Nominal power | P_m | 2.2 kW |
| | Nominal wind power | V_{w-nom} | 12m\ s |
| | Base rotational speed | W_{m-base} | 462\ 322 |
| | Maximum value of | C_{pmax} | 0.48 |

chosen as the final solution after 20 runs of implementation.

The robustness of the MPPT built using GWO is demonstrated by its ability to collect the most power from wind production systems installed in various locales. The outcomes in each of the scenarios under study supported the developed tracker's superiority

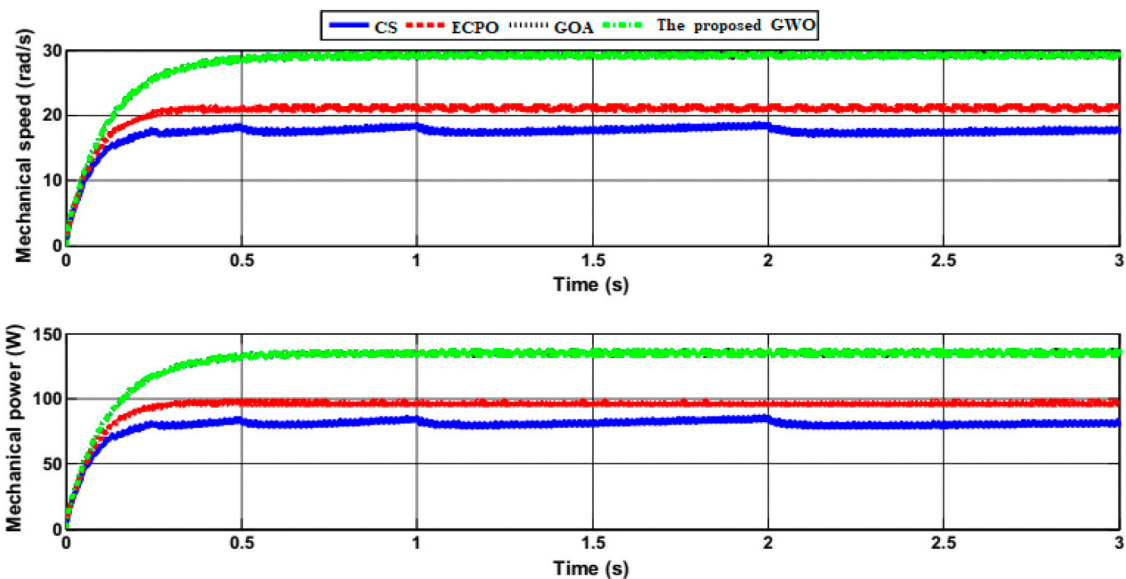


Figure 4. At $V = 12$ m/s, the time responses of mechanical speed and power.

and dependability thanks to the suggested GWO-based approach. As a result of its ability to operate in online mode, the authors advise the installation of GWO-MPPT with wind energy producing systems (Figures 4 and 5).

The proposed GWO is practised, and the outcomes are evaluated against electric charged particle optimization (ECPO), grasshopper optimization algorithm (GOA) and cuckoo search (CS). The best outcomes in this situation are shown in Table 3. With a maximum

Table 3. The results gathered through the proposed GWO and the others at $V = 12$ m/s.

| | CS | GOA | ECPO | Proposed GWO |
|-----------------|---------|---------|---------|--------------|
| p_m (W) | 81.3745 | 143.816 | 89.237 | 143.829 |
| w_m (rad/sec) | 17.7283 | 30.373 | 21.816 | 30.421 |
| duty | 0.3001 | 0.0939 | 0.1572 | 0.0932 |
| p_{max} (W) | 73.134 | 103.885 | 81.214 | 103.418 |
| V_{MPP} (V) | 134.23 | 165.426 | 141.871 | 165.871 |
| I_{MPP} (A) | 0.2314 | 0.8754 | 0.2198 | 0.8934 |

Table 4. Comparison of various research methodology.

| S.no | Author & year | Description | Outcome |
|------|---------------------------------------|--|--|
| 1 | Oussama Hachana et al. year:2022 | Shuffled complex evolution optimizer for an effective PMSG WT using control of energy storage system | The outcome show that the SCE algorithm outperforms classic SMC and competing algorithms in terms of active power steady-state error (0.832%), rise time (1.8245 104s), peak value (6.985 103 W), overall efficiency (98.9100%) and total harmonic distortion (0.9100%). |
| 2 | Mohammad Junaid Khan et al. year:2022 | Real-time adaptive MPPT for WT systems using an AIAPOMPPT controller | To enhance the outcomes and compare power variations on MPPT with changeable wind speed, the proposed algorithm is utilized. |
| 3 | Ahmed Fathy et al. year:2022 | Wind energy producing system maximum power point tracker based on the Archimedes optimization method | The outcomes demonstrated the effectiveness of the AOA-MPPT controller in optimizing the performance of the WECS, outperforming all other optimizers that were taken into consideration. |
| 4 | Kunlun Han et al. year:2021 | Algorithm for controller parameter optimization using WT based on doubly-fed induction generators that have been optimized | Improve the DFIG-based wind power system's average power coefficient by at least 0.0028% when compared to other algorithms. |
| 5 | Hamid Chojaa et al. year:2021 | Under an actual wind profile, integral sliding mode control for DFIG-based WECS with MPPT is implemented. | The efficiency and durability of every control technique have been built and examined in a MATLAB/Simulink using 1.6 MW wind system model. |
| 6 | AliDarvish Falehi et al. year:2020 | Multi-purpose grasshopper optimization algorithm-based RPO-FOSMC for DFIG-based WT will improve MPPT and FRT capabilities. | The proper perturbation observer has assessed the stochastic response of wind speed as well as the non-linearity and instability of the DFIG parameters. |
| 7 | Irfan Yazıcı et al. year:2020 | modified MPPT algorithm for the WECS using golden section search | Comparative investigations support the superiority of the suggested strategy over traditional and variable step P&Q technique in terms of MPP extracted from the system. |
| 8 | Proposed | MPPT design utilizing grey wolf optimization technique for WECS | In the near future, the suggested method will be used to resolve a number of optimization issues for different renewable energy systems and the smart grid. |

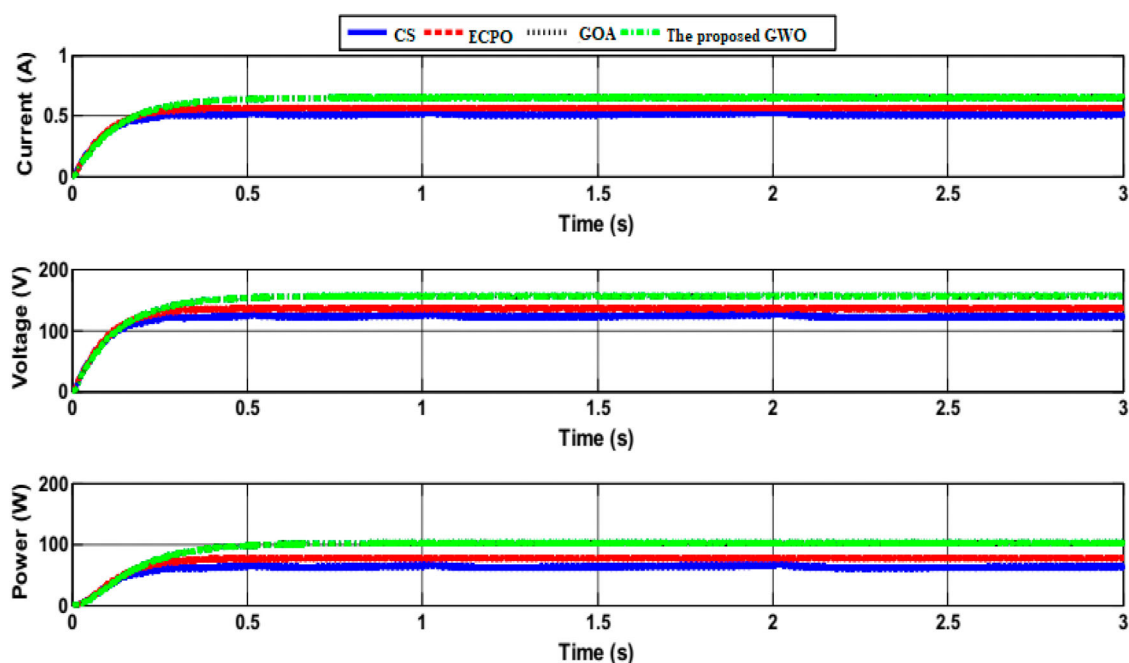


Figure 5. At $V = 12$ m/s, the time responses of current, voltage and electrical power.

electrical output of 143.829 W at a duty cycle of 0.0939 delivered to the converter MOSFET, the proposed GWO outperformed CS, GOA and ECPO. After feeding the converter with a duty cycle of 0.0932. Maximum outputs of 63.5237 and 78.3044 W were attained by CS and ECPO-based algorithms, respectively, with duty cycles of 0.2 and 0.1576. This demonstrates that local optima exist for both CS and ECPO (Table 4).

5. Conclusion

In this study, a unique application of the GWO was used to develop the MPPT integrated with the wind energy producing system and enhance performance. This study suggests an adaptive fuzzy-based MPPT method for precise and successful tracking. In the generation system being exhibited, WT and PMSG are coupled. The proposed GWO's management of the converter MOSFET's duty cycle optimizes the output power from the WECS. The recommended GWO-MPPT controller extracts 102.136 W when used with variable speed, compared to 101.7 W from the GOA MPPT controller. The results showed that the suggested GWO-MPPT controller outperformed all other optimizers that were taken into account in terms of improving the efficiency of the wind energy producing system. The suggested approach will be applied in the near future to address a number of optimization issues for various renewable energy systems and the smart grid.

Disclosure statement

No potential conflict of interest was reported by the author(s).

References

- [1] Liang R-H, Liao J-H. A fuzzy-optimization approach for generation scheduling with wind and solar energy systems. *IEEE Trans Power Syst.* 2007;22(4):1665–1674.
- [2] Saber AY, Venayagamoorthy GK. Efficient utilization of renewable energy sources by gridable vehicles in cyber-physical energy systems. *IEEE Syst J.* 2010;4(3):285–294.
- [3] Bataineh KM, Dalalah D. Assessment of wind energy potential for selected areas in Jordan. *Renew Energy.* 2013;59:75–81.
- [4] Nikolova S, Causevski A, Al-Salaymeh A. Optimal operation of conventional power plants in power system with integrated renewable energy sources. *Energy Convers Manage.* 2013;65:697–703.
- [5] Michalak P, Zimny J. Wind energy development in the world, Europe and Poland from 1995 to 2009; current status and future perspectives. *Renew Sustain Energy Rev.* 2011;15(5):2330–2341.
- [6] Luo X, Niu S. A novel contra-rotating power split transmission system for wind power generation and its dual MPPT control strategy. *IEEE Trans Power Electron.* 2016;32(9):6924–6935.
- [7] Wu A, Zhao B, Mao J, et al. Adaptive active fault-tolerant MPPT control for wind power generation system under partial loss of actuator effectiveness. *Int J Electr Power Energy Syst.* 2019;105:660–670.
- [8] Sreenivas P, Srinivasa Murthy VS, Vijaya Kumar S, et al. Design and analysis of new pitch angle controller for enhancing the performance of wind turbine coupled with PMSG. *Mater Today Proc.* 2022;52(Part 3):1456–1460. ISSN 2214-7853.
- [9] Hachana O, Meghni B, Benamor A, et al. Efficient PMSG wind turbine with energy storage system control based shuffled complex evolution optimizer. *ISA Trans.* 2022;131:377–396. ISSN 0019-0578.
- [10] Zholtayev D, Rubagotti M, Do TD. Adaptive super-twisting sliding mode control for maximum power point tracking of PMSG-based wind energy conversion systems. *Renewable Energy.* 2022;183:877–889. ISSN 0960-1481.
- [11] Fathy A, Alharbi AG, Alshammari S, et al. Archimedes optimization algorithm based maximum power point tracker for wind energy generation system. *Ain Shams Engineering Journal.* 2022;13(2):101548. ISSN 2090-4479.
- [12] Han K, Huang T, Yin L. Quantum parallel multi-layer Monte Carlo optimization algorithm for controller parameters optimization of doubly-fed induction generator-based wind turbines. *Appl Soft Comput.* 2021;112:107813. ISSN 1568-4946.
- [13] Yin L, Gao Q. Multi-objective proportional-integral-derivative optimization algorithm for parameters optimization of double-fed induction generator-based wind turbines. *Appl Soft Comput.* 2021;110(2021):107673. ISSN 1568-4946.
- [14] Choja H, Derouich A, Chehaidia SE, et al. Integral sliding mode control for DFIG based WECS with MPPT based on artificial neural network under a real wind profile. *Energy Reports.* 2021;7:4809–4824. ISSN 2352-4847.
- [15] Sitharthan R, Karthikeyan M, Sundar DS, et al. Adaptive hybrid intelligent MPPT controller to approximate effectual wind speed and optimal rotor speed of variable speed wind turbine. *ISA Trans.* 2020;96:479–489.
- [16] Kumar AP, Parimi AM, Uma Rao K. Implementation of MPPT control using fuzzy logic in solar-wind hybrid power system. In: 2015 IEEE international conference on signal processing, informatics, communication and energy systems (SPICES); 2015. p. 1–5.
- [17] Priyadarshi N, Ramachandaramurthy VK, Padmanaban S, et al. An ant colony optimized MPPT for standalone hybrid PV-wind power system with single Cuk converter. *Energies.* 2019;12(1):167.
- [18] Oussama M, Abdelghani C, Lakhdar C. Efficiency and robustness of type-2 fractional fuzzy PID design using salps swarm algorithm for a wind turbine control under uncertainty. *ISA Trans.* 2022;125:72–84. ISSN 0019-0578.
- [19] Tang X-Y, Yang Q, Stoevesandt B, et al. Optimization of wind farm layout with optimum coordination of turbine cooperations. *Comput Ind Eng.* 2022;164:107880. ISSN 0360-8352.
- [20] Khan MJ. An AIAPO MPPT controller based real time adaptive maximum power point tracking technique for wind turbine system. *ISA Trans.* 2022;123:492–504. ISSN 0019-0578.